HHS Public Access

Author manuscript

Cancer Cell. Author manuscript; available in PMC 2017 April 11.

Published in final edited form as:

Cancer Cell. 2016 April 11; 29(4): 536–547. doi:10.1016/j.ccell.2016.03.001.

N-Myc Drives Neuroendocrine Prostate Cancer Initiated from Human Prostate Epithelial Cells

John K. Lee[1,2], **John W. Phillips**[3], **Bryan A. Smith**[3], **Jung Wook Park**[3], **Tanya Stoyanova**[3], **Erin F. McCaffrey**[3], **Robert Baertsch**[4], **Artem Sokolov**[4], **Justin G. Meyerowitz**[5,6,7], **Colleen Mathis**[3], **Donghui Cheng**[8], **Joshua M. Stuart**[4], **Kevan M. Shokat**[5,7,12], **W. Clay Gustafson**[5,9], **Jiaoti Huang**[8,10], and **Owen N. Witte**[3,8,11,12,*]

[1]Division of Hematology and Oncology, Department of Medicine, University of California, Los, Angeles, Los Angeles, CA 90095, USA

[2]Molecular Biology Institute, University of California, Los Angeles, Los Angeles, CA 90095, USA

[3]Department of Microbiology, Immunology, and Medical Genetics, University of California, Los, Angeles, Los Angeles, CA 90095, USA

[4]Center for Biomolecular Science and Engineering, Jack Baskin School of Engineering, University of California, Santa Cruz, Santa Cruz, CA 95064, USA

[5]Helen Diller Family Comprehensive Cancer Center, University of California, San Francisco, San Francisco, CA 94158, USA

[6]Departments of Neurology and Neurological Surgery, University of California, San Francisco, San Francisco, CA 94158, USA

[7]Department of Cellular and Molecular Pharmacology, University of California, San Francisco, San Francisco, CA 94158, USA

[8]Eli and Edythe Broad Center of Regenerative Medicine and Stem Cell Research, University of California, Los Angeles, Los Angeles, CA 90095, USA

[9]Department of Pediatrics, UCSF Benioff Children's Hospital, University of California, San Francisco, San Francisco, CA 94158, USA

[10]Department of Pathology and Laboratory Medicine, University of California, Los Angeles, Los, Angeles, CA 90095, USA

[*]Correspondence: owenwitte@mednet.ucla.edu (O.N.W.).

ACCESSION NUMBERS

The RNA-Seq and aCGH data reported in this paper have been deposited in NCBI GEO: GSE77624 and GSE77368.

AUTHOR CONTRIBUTIONS

J.K.L. and O.N.W. conceived the project; J.K.L, J.W.P., B.A.S., J.W.P., T.S., E.F.M., and W.C.G. performed the experiments; R.B., A.S., J.G.M, J.M.S., K.M.S., W.C.G. and J.H. assisted with data interpretation; C.M. and D.C. provided technical assistance with human tissue processing; J.K.L. and O.N.W. wrote the manuscript.

[11]Department of Molecular and Medical Pharmacology, University of California, Los Angeles, Los Angeles, CA 90095, USA

[12]Howard Hughes Medical Institute, University of California, Los Angeles, Los Angeles, CA, 90095, USA

SUMMARY

MYCN amplification and overexpression are common in neuroendocrine prostate cancer (NEPC). However, the impact of aberrant N-Myc expression in prostate tumorigenesis and the cellular origin of NEPC have not been established. We define N-Myc and activated AKT1 as oncogenic components sufficient to transform human prostate epithelial cells to prostate adenocarcinoma and NEPC with phenotypic and molecular features of aggressive, late-stage human disease. We directly show that prostate adenocarcinoma and NEPC can arise from a common epithelial clone. Further, N-Myc is required for tumor maintenance and destabilization of N-Myc through Aurora A kinase inhibition reduces tumor burden. Our findings establish N-Myc as a driver of NEPC and a target for therapeutic intervention.

INTRODUCTION

NEPC makes up less than 2% of all primary prostate cancers (Helpap et al., 1999). However, treatment-related NEPC often emerges during androgen deprivation therapy for prostate adenocarcinoma, the predominant subtype of prostate cancer (Beltran et al., 2014). The term NEPC describes a heterogeneous group of neuroendocrine tumors defined morphologically that include well-differentiated carcinoid, adenocarcinoma with neuroendocrine differentiation, adenocarcinoma with Paneth cell-like neuroendocrine differentiation, mixed neuroendocrine carcinoma-acinar adenocarcinoma, and the more aggressive large cell carcinoma and small cell carcinoma (Epstein et al., 2014). NEPC is also distinguished from prostate adenocarcinoma by the expression of neuroendocrine differentiation markers and the loss of expression of the androgen receptor (AR) and prostate-specific antigen (PSA) (Wang and Epstein, 2008). Patients with aggressive NEPC have limited treatment options and succumb to the disease within a year (Spiess et al., 2007).

Aggressive NEPC represents a lethal endpoint in the progression of prostate cancer from prostate adenocarcinoma to castration-resistant prostate cancer (CRPC) to NEPC. Neuroendocrine transdifferentiation is an adaptive mechanism of resistance to androgen withdrawal observed *in vitro* and *in vivo* (Lin et al., 2014; Shen et al., 1997). The phenotypic conversion to NEPC is associated with recurrent genetic lesions including mutation or deletion of *RB1* and *TP53* as well as the overexpression and genomic amplification of *MYCN* and *AURKA* (Beltran et al., 2011; Tan et al., 2014). NEPCs also harbor genetic abnormalities present in prostate adenocarcinomas such as *ETS* rearrangements and *PTEN* mutations (Beltran et al., 2011; Tan et al., 2014), indicating that these cancer types may arise from a common clonal origin.

Prior work has identified multipotent stem and progenitor cells within the basal epithelial compartment of the mouse and human prostate that give rise to basal, luminal, and neuroendocrine cells (Goldstein et al., 2010; Goldstein et al., 2008). Others have shown

through lineage tracing studies that both basal and luminal cells in the mouse prostate can be cell types of origin of cancer (Choi et al., 2012; Wang et al., 2009). Importantly, we have demonstrated that naïve basal cells in the human prostate can serve as targets of direct transformation. The overexpression of ERG and constitutively active myristoylated AKT1 (myrAKT1) initiated prostate cancer from human prostate basal cells (Goldstein et al., 2010). Loss of the tumor suppressor PTEN is found in 70% of prostate cancers and leads to the activation of AKT1, a common early event in prostate cancer tumorigenesis (Gray et al., 1998; Wu et al., 1998). Further studies showed that the deregulated expression of c-Myc and myrAKT1 in human basal cells generated prostate adenocarcinoma and squamous cell carcinoma from a common precursor (Stoyanova et al., 2013). The c-Myc/myrAKT1 human prostate cancer model highlights the potential for biphenotypic tumors to arise from divergent differentiation during tumorigenesis.

The Myc family of proto-oncogenes (*MYC, MYCL*, and *MYCN*) encodes a group of multifunctional transcription factors whose deregulation plays a role in the initiation and maintenance of most human cancers (Dang, 2012). *MYC* is commonly overexpressed and amplified in prostate cancer (Fleming et al., 1986; Jenkins et al., 1997). A recent study has demonstrated recurrent, focal amplification of *MYCL* in 27% of localized prostate cancers (Boutros et al., 2015). *MYCN* has been shown to be overexpressed and amplified in approximately 40% of NEPCs but only 5% of prostate adenocarcinomas (Beltran et al., 2011). Numerous studies have implicated N-Myc as a critical oncoprotein required for the development of neural and neuroendocrine tumors (Beltran, 2014). Here, we sought to evaluate the functional role of N-Myc in the initiation and maintenance of human NEPC.

RESULTS

N-Myc and myrAKT1 Overexpression in Human Prostate Basal Cells Initiates NEPC and Prostate Adenocarcinoma

To investigate whether N-Myc can initiate prostate cancer from human prostate epithelial cells, we used a tissue regeneration model of prostate cancer developed by our group (Figure 1A) (Goldstein et al., 2010; Stoyanova et al., 2013). Benign regions of prostate tissue from patients undergoing prostatectomy were dissociated to single cells. Basal epithelial cells were purified based on cell surface markers ($CD45^{-}Trop2^{+}CD49f^{hi}$). AKT1 was introduced as a sensitizing oncogenic event as it is frequently activated in prostate cancers including NEPCs (Figure 1D) and the overexpression of myrAKT1 initiates pre-malignant prostatic intraepithelial neoplasia in our human prostate transformation assay (Stoyanova et al., 2013). Enforced expression of N-Myc and activated AKT1 in the epithelial cells was achieved by lentiviral transduction. Transduced epithelial cells were mixed with mouse urogenital sinus mesenchyme (UGSM) and implanted subcutaneously in NOD-SCID-IL2Rγ^{null} (NSG) mice supplemented with testosterone.

The overexpression of N-Myc and myrAKT1 in sets of prostate basal cells from five human prostatectomy specimens (Table S1) produced tumors (Figure 1B) after 6–10 weeks with no evidence of metastatic disease. Histology of the N-Myc/myrAKT1 tumors revealed regions of high-grade adenocarcinoma and infrequent squamous cell carcinoma like the human c-Myc/myrAKT1 tumors described previously (Stoyanova et al., 2013). Some regions

exhibited high nuclear-to-cytoplasmic ratio, frequent mitotic figures, and apoptotic features consistent with NEPC, including areas of small cell prostate carcinoma (SCPC) (Figures 1C and S1A) (Wang and Epstein, 2008). Other regions of the tumors were consistent with mixed neuroendocrine carcinoma-acinar adenocarcinoma (Figure 2B). The tumors expressed N-Myc and activated AKT1 (Figure 1D) and their human origin was confirmed by immunostaining for human leukocyte antigen (HLA) Class I ABC (Figure S1C). N-Myc/myrAKT1 tumors also expressed the luminal marker cytokeratin 8 (CK8) but lacked the basal marker p63 (Figure 1E), indicating loss of the basal cell layer which is a hallmark of prostate cancer.

To evaluate whether luminal prostate epithelial cells could also be transformed by N-Myc and myrAKT1, we isolated luminal cells from four benign human prostates based on cell surface markers ($CD45^{-}Trop2^{+}CD49f^{low}$) and transduced them in a comparable manner. Similar to prior studies (Goldstein et al., 2010; Stoyanova et al., 2013), human luminal cells did not produce tumors after oncogenic challenge (data not shown).

While the diagnosis of NEPC is usually made by the recognition of classic histologic features, assessment of neuroendocrine marker expression by immunohistochemistry (IHC) is often performed to confirm the clinical diagnosis (Epstein et al., 2014). The neuroendocrine carcinoma in the N-Myc/myrAKT1 tumors demonstrated expression of neural cell adhesion molecule 1 (NCAM1), chromogranin A (CHGA), synaptophysin (SYP), thyroid transcription factor-1 (TTF-1), and forkhead box A2 (FOXA2) (Mirosevich et al., 2006; Yao et al., 2006). We detected immunostaining of these proteins in the regions of neuroendocrine carcinoma but not of adenocarcinoma in the N-Myc/myrAKT1 tumors (Figures 2A–C). While all tumors showed morphologic evidence of NEPC, the expression pattern of the neuroendocrine markers was heterogeneous with only one tumor expressing all five markers (Figure 2D). This heterogeneity in expression of markers is similar to what is appreciated in human NEPC specimens (Yao et al., 2006).

N-Myc/myrAKT1 Tumors Are Castration-Resistant

An invariant feature of late-stage human prostate cancer including NEPC is castration-resistant proliferation. The N-Myc/myrAKT1 tumors exhibited absent AR expression by IHC (Figure 2A), by immunoblotting (Figure 2E), and by gene expression (Figure 4D). We assessed the functional dependence of N-Myc/myrAKT1 tumor growth on androgens by subcutaneously injecting the $CD49f^{low}$ tumor cells in intact or castrate animals. Passage of $CD49f^{low}$ cells (Stoyanova et al., 2013) from N-Myc/myrAKT1 tumors gave rise to tumors demonstrating mixed neuroendocrine carcinoma and adenocarcinoma (Figure S1B). No difference in the growth kinetics of the tumors was observed in intact and castrate hosts (Figure 3A), indicating that the N-Myc/myrAKT1 tumors are castration-resistant. In contrast, the androgen-dependent human prostate cancer cell line LNCaP formed tumors in intact animals but showed no growth in castrate animals (Figure 3A).

The histology of the N-Myc/myrAKT1 tumors passaged in castrate mice also showed mixed neuroendocrine carcinoma and adenocarcinoma on a background of necrosis (Figure S1B). To quantify the relative percentage of each cancer subtype by area in the tumors, we implemented smart image segmentation to differentiate neuroendocrine carcinoma and

adenocarcinoma on H&E-stained sections (Figure S2A–C). We noted a progressive enrichment of the neuroendocrine carcinoma within the tumor with successive passage in castrate mice, from 9% in the primary tumor to 28% in the tertiary tumor (Figure 3B). These results suggest a statistically significant but subtle competitive advantage of NEPC upon serial propagation in castrate conditions.

N-Myc/myrAKT1 Tumors Are Invasive and Metastatic

To gauge the metastatic potential of the N-Myc/myrAKT1 tumors, we first used a tail vein assay to model the invasion-metastasis cascade (Valastyan and Weinberg, 2011). As a source of tumor cells, we dissociated an N-Myc/myrAKT1 tumor to single cells and propagated them in HITES media (Carney et al., 1981). N-Myc/myrAKT1 tumor cells and the non-metastatic human prostate cancer cell line LNCaP were transduced with a lentivirus expressing firefly luciferase (Luc) to produce the N-Myc/myrAKT1-Luc and LNCaP-Luc sublines. Tumor cells were injected into the tail veins of NSG mice. Bioluminescence was detected in the hindlimbs and pelvis in two of three N-Myc/myrAKT1-Luc mice on day 21 whereas signal was absent in LNCaP-Luc mice (Figure 3C). Necropsy of the mice showed tumors involving limb bones, sacrum, and liver (Figure 3D). We did not appreciate macrometastatic disease in the lungs despite bioluminescent imaging showing localization of N-Myc/myrAKT1-Luc cells to the lungs immediately after tail vein injection (Figure S2D). However, microscopic review of lung sections revealed numerous foci of micrometastatic disease (Figure S2E).

To confirm these findings, we performed an orthotopic injection assay of metastasis which necessitates local invasion and intravasation, in addition to metastatic processes required for the tail vein assay. N-Myc/myrAKT1-Luc or LNCaP-Luc tumor cells were implanted into the left lateral lobes of the prostates of NSG mice. Mice were sacrificed on day 74 because of abdominal distention of the N-Myc/myrAKT1-Luc mice. Imaging prior to euthanasia revealed multiple areas of bioluminescence in three of three N-Myc/myrAKT1-Luc mice while signal was confined to the prostate in LNCaP-Luc mice (Figure 3E). Necropsy of the N-Myc/myrAKT1-Luc mice showed extensive disease in lymph nodes and vital organs including liver and kidney (Figure 3F).

The tumors from the metastasis models exhibited a mixed phenotype of neuroendocrine carcinoma and adenocarcinoma identical to the parental tumor (Figures 3G–H). They also retained expression of the linked fluorescent markers from the N-Myc and myrAKT1 proviruses, HLA Class I ABC, and the neuroendocrine marker FOXA2 (Figures S2F–G). Collectively, these findings indicate that N-Myc/myrAKT1 tumor cells are highly aggressive and proficient in the multi-step process of metastatic dissemination.

Molecular Characterization of N-Myc/myrAKT1 Tumors

We then questioned whether the N-Myc/myrAKT1 tumors demonstrated molecular properties of human NEPC. Previously, Beltran *et al.* analyzed seven NEPCs (five SCPCs) and 30 prostate adenocarcinomas by next-generation RNA sequencing (RNA-Seq) to illustrate gene networks involving AR signaling, neuroendocrine processes, and cell cycle regulation that distinguish these entities (Beltran et al., 2011). To evaluate global

transcriptome features in the N-Myc/myrAKT1 tumors, we harvested three N-Myc/myrAKT1 tumors, isolated regions of neuroendocrine carcinoma and adenocarcinoma from frozen sections by laser capture microdissection, and processed the specimens for RNA-Seq analysis (Figure 4A).

Within each of the tumors, we identified fewer than 1500 genes differentially expressed (>4-fold) between the neuroendocrine carcinoma and adenocarcinoma. Gene set enrichment analysis of differentially expressed genes (>4-fold) in the N-Myc/myrAKT1 tumor derived from Patient 1 showed enrichment for neuronal pathways including targets of *NRSF/REST*, a master repressor of neural genes (Chong et al., 1995), in the neuroendocrine carcinoma (Figure 4B). The adenocarcinoma was enriched in stem cell-associated pathways involving *BMI1, SHH, NANOG*, and *WNT*. On the other hand, the neuroendocrine carcinoma and adenocarcinoma components of the N-Myc/myrAKT1 tumors generated from Patient 2 and 4 showed differential expression (>4-fold) of only 114 and 80 genes.

We generated a weighted 50-gene predictor to identify the gene expression features that most discriminate neuroendocrine prostate cancers from prostate adenocarcinomas in the Beltran *et al*. dataset (Table S2). Gene ontology of this NEPC gene signature identified biological processes like secretion, neurotransmitter transport, neuron differentiation, and glial and oligodendrocyte fate. The predictor was applied to the N-Myc/myrAKT1 tumors to derive gene signature scores that approximate their likeness to neuroendocrine prostate cancer. Both the neuroendocrine carcinoma and adenocarcinoma components of the N-Myc/myrAKT1 tumors scored positively but intermediate in value to the Beltran *et al*. tumors (Figure 4C).

Like the NEPCs profiled by Beltran *et al*., both components of the N-Myc/myrAKT1 tumors showed low levels of expression of the epithelial marker *TACSTD2, AR*, and the androgen-regulated genes *NKX3-1, KLK3*, and *TMPRSS2* (Figure 4D). Consistent with our IHC results, expression of the neuroendocrine markers *CHGA, SYP, NCAM1*, and *ENO2* was heterogeneous (Figures 2D and 4D). *MYCN* was highly expressed from the integrated proviruses in the N-Myc/myrAKT1 tumors. We also identified elevated levels of the cell cycle regulation gene *AURKA* (Beltran et al., 2011; Mosquera et al., 2013). Our gene expression analysis also demonstrated that the polycomb genes *CBX2* and *EZH2* and other recently identified NEPC epigenetic regulators (Clermont et al., 2015) are upregulated in the N-Myc/myrAKT1 tumors and the Beltran *et al*. NEPCs (Figure 4D). These results show that the N-Myc/myrAKT1 tumors exhibit many of the defining molecular attributes that exemplify human NEPC.

To determine whether significant genomic abnormalities occur during progression to NEPC in our model, we performed high-resolution copy number analysis on three N-Myc/myrAKT1 tumors by array comparative genomic hybridization (aCGH). Two tumors exhibited no large chromosomal anomalies while one tumor showed a gain in chromosome 7 (Figure S3 and Table S3). Copy number alterations were identified in more than one tumor but these mapped to genomic regions of copy number polymorphism based on the dbVar and DGVa databases (Table S3). These findings suggest that N-Myc and myrAKT1 drive the

transformation of human prostate epithelial cells to NEPC without the need for large-scale genetic abnormalities.

We also performed whole exome sequencing of the tumors with an average of ~70-fold coverage to evaluate for mutations acquired during tumorigenesis. We calculated a mutation rate of 3.5 per megabase which is higher than the 2.0 per megabase described in heavily treated CRPC (Grasso et al., 2012). This value may be inflated due to the lack of matched benign samples in our analysis and the dependence on single nucleotide polymorphism filters. Unique mutations were identified in *CCDC168, GLYAT, OR2W3, SMARCA2*, and *ZFPM1* in more than one tumor (Table S4). Loss of *SMARCA2*, a catalytic subunit of the SWI/SNF chromatin remodeling complex, promotes androgen-independent proliferation in mouse prostate epithelial cells via E2F1 (E2F transcription factor 1) deregulation (Shen et al., 2008). Our analysis did not reveal mutations in genes altered at high frequency in advanced prostate cancer such as *AR, TP53, RB1*, and *FOXA1* (Grasso et al., 2012).

Human N-Myc/myrAKT1 Prostate Cancer Cells Are Highly Tumorigenic and Demonstrate Plasticity

The propagation of N-Myc/myrAKT1 tumor cells *in vitro* led to the establishment of a cell line named LASCPC-01. These cells grow rapidly in suspension (doubling time ~18 hours) as floating and attached clusters reminiscent of small cell lung cancer cell lines (Figure 5A) (Carney et al., 1981). Immunoblot analysis of LASCPC-01 cells showed expression of N-Myc and activated AKT1, AURKA, and the neuroendocrine markers ASCL1 and NSE (Figure 5B). ASCL1 is a pro-neural transcription factor expressed in NEPC (Rapa et al., 2008). Conventional karyotyping of LASCPC-01 cells showed a 46 X,Y male karyotype without chromosomal abnormalities (Figure 5C). Copy number analysis of the LASCPC-01 cell line revealed a mosaic gain of 1q23.1-1q44 (Figure S3 and Table S3).

To evaluate the capacity of N-Myc/myrAKT1 prostate cancer cells to propagate tumors, we performed a limiting dilution xenograft assay (Figure 5D). We estimated that 1 in 6.5 cells (95% CI 2.8–14.9) exhibited tumor regenerative capacity (Hu and Smyth, 2009). In all tumors, including those from singly xenografted N-Myc/myrAKT1 tumor cells, we discovered mixed neuroendocrine carcinoma and adenocarcinoma similar to the parental N-Myc/myrAKT1 tumor (Figures 5E, S1A, and S4A). This finding suggested that a single N-Myc/myrAKT1 tumor clone could give rise to neuroendocrine carcinoma and adenocarcinoma.

To confirm this observation, we performed single cell sorting to expand individual N-Myc/myrAKT1 tumor cell clones from the LASCPC-01 cell line (Figure 5F). Eleven clonal sublines of LASCPC-01 were subcutaneously xenografted in NSG mice and generated tumors in four weeks (Figure 5F). Histologic examination showed that all clonal subline xenograft tumors exhibited both neuroendocrine carcinoma and adenocarcinoma phenotypes (Figures 5G and S4B). These results indicate that N-Myc and myrAKT1 cooperate to produce cancer cells marked by high tumor propagating potential and the capacity to generate biphenotypic prostate tumors.

N-Myc Expression Is Essential for Tumor Maintenance in N-Myc/myrAKT1 Tumors

We next questioned whether N-Myc expression is required for tumor maintenance. Studies in *MYC*-driven mouse models of osteogenic sarcoma, lymphoma, and hepatocellular carcinoma have shown that inactivation of c-Myc reverses tumorigenesis through the induction of proliferative arrest, differentiation, cellular senescence and apoptosis (Jain et al., 2002; Wu et al., 2007). To address the question of N-Myc dependence, we used a lentivirus with doxycycline-inducible N-Myc expression and a lentivirus with constitutive myrAKT1 expression (Figure 6A) in our tissue regeneration model of prostate cancer (Figure 1A). Eight weeks after implantation of the graft in an NSG mouse supplemented with a doxycycline diet, we harvested an inducible N-Myc/myrAKT1 tumor with the same histologic features of mixed NEPC as the constitutive N-Myc/myrAKT1 tumors (Figures 6B and S1A).

While dissociated cells from the inducible N-Myc/myrAKT1 tumor propagated tumors in mice fed doxycycline, they did not form tumors in mice that were not fed doxycycline (Figure 6C). In mice that were initially supplemented with doxycycline and allowed to establish inducible N-Myc/myrAKT1 tumors, doxycycline withdrawal led to a rapid and significant regression of the tumors within 96 hours (Figure 6C). Immunoblot analysis of these tumors after doxycycline withdrawal revealed a dramatic decrease in N-Myc protein levels (Figure 6D). Further, histologic evaluation of the tumors 72 hours after doxycycline withdrawal showed significant necrosis with a remarkable decline in cellularity (Figure 6E). These results demonstrate that N-Myc is necessary for tumor maintenance in our human transformation model of NEPC and suggest that N-Myc is an important therapeutic target in *MYCN*-amplified NEPC.

Pharmacologic Inhibition of N-Myc Dependence in NEPC

AURKA expression in the N-Myc/myrAKT1 tumors (Figure 4D) and LASCPC-01 cell line (Figure 5B) is consistent with the concept of a feed-forward loop between N-Myc and AURKA identified in childhood neuroblastoma (Otto et al., 2009). N-Myc induces the expression of AURKA and AURKA regulates the stability of N-Myc through a kinase-independent protein interaction with N-Myc and the Fbxw7 ubiquitin ligase that prevents N-Myc proteolysis. Treatment of *MYCN*-amplified neuroblastoma cell lines with the Aurora A kinase inhibitor MLN8237 reduced N-Myc protein levels by up to 60% and suppressed growth (Brockmann et al., 2013). MLN8237 is now being evaluated in a clinical trial for NEPC (Beltran et al., 2011). Recently, a class of conformation-disrupting (CD) AURKA inhibitors was designed and optimized to potently destabilize N-Myc (Gustafson et al., 2014). The lead compound, CD532, directly interacts with AURKA and induces a global conformational shift, disrupting the AURKA/N-Myc protein complex and promoting the degradation of N-Myc by the ubiquitin-proteasome pathway. Further, the cytotoxic activity of CD532 was evaluated in human cancer cell lines and sensitivity to CD532 strongly correlated with amplification and expression of *MYCN*. Human prostate cancer cell lines were not tested.

We therefore sought to test CD532 in our N-Myc/myrAKT1 prostate cancer model to evaluate its therapeutic potential in NEPC. After three hours of treatment with CD532,

LASCPC-01 cells showed a dose-dependent decline in N-Myc protein levels, inhibition of Aurora A kinase activity (phosphorylation of histone H3), and induction of cleaved PARP (Figure 7A). Diminished N-Myc protein expression was identified in LASCPC-01 cells treated with CD532 at doses of 250 nM and greater. On the other hand, treatment with the pan-Aurora kinase inhibitor VX-680 and MLN8237 did not reduce N-Myc protein levels over the same timeframe (Figure 7B) and across a range of doses and time points (Figure S5A), showing differences in the ability of these AURKA inhibitors to destabilize N-Myc and inhibit Aurora A kinase activity. CD532 induced a log reduction in LASCPC-01 cell viability at three hours (Figure 7C) coincident with a rapid decline in N-Myc protein levels and accompanied by increased cleaved caspase-3 (Figure 7D). Cell cycle analysis also confirmed a significantly increased sub-G1 population consistent with cell death (Figure 7E). Treatment with MLN8237 or cabazitaxel, a taxane approved for the treatment of metastatic CRPC, showed minimal early effects relative to DMSO treatment (Figures 7C and 7E).

The half-maximal effective concentration (EC50) of CD532 in LASCPC-01 cells was 99.4 nM (95% CI: 81.7–120.8 nM) at 48 hours (Figure 7F). In contrast, the EC50s of the LNCaP and DU145 human prostate cancer cell lines were approximately 20-fold higher (Figure S5B). These findings suggest that the inhibitory effect of CD532 is more specific for N-Myc-driven prostate cancer. To show that the ubiquitin-proteasome pathway is critical for N-Myc destabilization by CD532, LASCPC-01 cells were treated with a dose range of CD532 and the proteasomal inhibitor MG-132. MG-132 stabilized N-Myc but did not affect the inhibition of Aurora A kinase activity (Figure S5C).

We also assessed the human kinome interaction profile of CD532 using an active site-directed competition binding assay to characterize off-target interactions (Karaman et al., 2008). Aside from AURKA, CD532 kinase interactors include cyclin-dependent kinases like CDK2 and CDK7, KIT, FLT3, PDGFRB, RET, and FGF receptors (Figure S5D and Table S5). Inhibition of these targets may potentiate the N-Myc destabilizing effects of CD532. Relative to clinical kinase inhibitors, CD532 exhibited a favorable kinase selectivity profile comparable to crizotinib (Figure S5E).

To examine the *in vivo* effect of CD532, mice harboring passaged N-Myc/myrAKT1 tumors derived from two individual patient samples were treated with either vehicle or CD532 60 mg/kg daily for two doses. To confirm the on-target effect of CD532, the tumors were harvested and assayed for N-Myc expression normalized to GAPDH expression. CD532-treated tumors exhibited a 31.3% mean reduction in N-Myc protein levels relative to vehicle-treated tumors (Figure 7G). Treatment of a larger cohort of mice bearing subcutaneous LASCPC-01 xenograft tumors with CD532 25 mg/kg twice per week significantly reduced tumor burden over vehicle treatment (Figure 7H). Our results show that disruption of N-Myc stability through AURKA inhibition in *MYCN*-amplified NEPC may be a rational and promising therapeutic strategy.

DISCUSSION

Models of NEPC have been limited to human tumor xenografts with poorly defined genetic drivers and genetically engineered mouse models (ie. TRAMP and prostate-specific conditional knockouts) that inactivate p53 and Rb (Berman-Booty and Knudsen, 2015). However, the protracted tumor latencies of these mouse models reflect the need for secondary oncogenic events to promote prostate tumorigenesis. In these systems, pinpointing the function of driver oncogenes that are activated during prostate cancer progression is challenging. We report that the deregulated expression of N-Myc and myrAKT1 in primary human prostate epithelial cells is sufficient to produce tumors with the characteristics of end-stage prostate cancer in the form of mixed NEPC and prostate adenocarcinoma. The abbreviated tumor latency and repeated observation of this phenotype in tumors derived from multiple unique human prostate samples indicate that N-Myc and activated AKT1 together are penetrant drivers of progression to NEPC.

Rapid castration-resistant proliferation and absence of AR expression are defining properties of the disease. N-Myc overexpression in the androgen-dependent LNCaP cell line has been shown to diminish AR expression levels (Beltran et al., 2011). The N-Myc/myrAKT1 tumors also showed low or absent AR expression and demonstrated primary androgen independence. These findings suggest that the acquisition of *MYCN* gene amplification and overexpression during prostate cancer evolution may allow escape from AR dependence and promote the emergence of CRPC and NEPC. Reciprocal regulation of c-Myc and AR expression has been described in prostate cancer (Gao et al., 2013; Ni et al., 2013) but the relationship between N-Myc and AR has not been explored.

Metastatic invasion of visceral organs is largely responsible for the exceedingly poor survival of patients with aggressive NEPC. N-Myc expression correlates with invasive and metastatic behavior in neuroblastoma and the N-Myc transcriptional program in neuroblastoma appears to regulate multiple aspects of metastasis (Huang and Weiss, 2013). While primary N-Myc/myrAKT1 tumors in the subcutaneous compartment did not demonstrate invasion or metastasis, dissociated tumor cells introduced into the tail veins or prostates of mice readily colonized bone, lymph nodes, and visceral organs. Although the microenvironment likely accounts for the absence of distant spread from the subcutaneous xenograft tumors (Stephenson et al., 1992), secondary genetic events and clonal selection during culture may have also contributed to the metastatic phenotype.

The cellular origin of NEPC has not been clearly defined. The prevailing hypothesis is that prostate adenocarcinomas undergo transdifferentiation to NEPC, especially under the selective pressure of androgen deprivation (Beltran et al., 2014; Lin et al., 2014; Shen et al., 1997). This theory is supported by genetic analyses of human prostate tumors with concurrent neuroendocrine carcinoma and adenocarcinoma where common *TP53* mutations and *TMPRSS2-ERG* rearrangements have been identified in both cancer types, suggesting a shared clonal origin (Hansel et al., 2009; Williamson et al., 2011). Our results functionally demonstrate that NEPC and prostate adenocarcinoma can both arise from a single N-Myc/myrAKT1 tumor cell clone derived from a prostate epithelial cell. Further, propagation of tumor cells in castrate conditions leads to enrichment of the NEPC over the prostate

adenocarcinoma. These findings show directly an epithelial-to-neuroendocrine transition and prove that a common clone gives rise to these cancer subtypes in human prostate cancer, as has been proposed by prior studies (Beltran et al., 2014; Lin et al., 2014). Our data suggest that a subset of primary prostate adenocarcinoma with *MYCN* amplification and overexpression may acquire cancer stem cell properties that allow them to act as lurking clones capable of repopulating the tumor with NEPC after treatment. Consistent with this idea, previous work has shown that concurrent *MYCN* and *AURKA* amplification was identified in 65% of prostate adenocarcinomas from patients who later developed NEPC but in only 5% from an unselected population (Mosquera et al., 2013).

Our collective studies do not rule out the possibility that a benign neuroendocrine cell could also be a target of transformation giving rise to NEPC. In small cell lung cancer, neuroendocrine cells and non-neuroendocrine epithelial cells have been found to be targets of transformation in a mouse model system, albeit with different efficiencies (Sutherland et al., 2011). Evaluation of this hypothesis in the human prostate with direct transformation studies is technically challenging due to the rarity of neuroendocrine cells in benign tissues and the lack of homogeneously expressed cell surface markers. In addition, we were unable to obtain outgrowths from human prostate luminal epithelial cells after introducing the oncogenes N-Myc and myrAKT1. This may reflect a limitation of our *in vivo* transformation assay as prior attempts to directly transform human luminal cells using this system have also been unsuccessful (Goldstein et al., 2010; Stoyanova et al., 2013). The advent of organoid cultures that enable the growth of luminal progenitor cells (Karthaus et al., 2014) may in the near future provide an opportunity to understand the functional impact of N-Myc overexpression and PI3K/AKT pathway activation in this population.

For decades, platinum-based chemotherapy has been the mainstay of treatment for aggressive human NEPC such as SCPC with dismal outcomes. In our studies, we functionally demonstrate that N-Myc drives NEPC and continuous expression of N-Myc is necessary for tumor maintenance. We propose that N-Myc is an attractive therapeutic target in this disease. Once considered impossible to target, the Myc family of oncoproteins can now be inhibited through a number of pharmacologic strategies (Dang, 2012). The positive feedback loop between N-Myc and Aurora A kinase identified in neuroblastoma (Otto et al., 2009) and NEPC (Beltran et al., 2011) provides one such opportunity. Our studies show that CD532 is highly active in our N-Myc/myrAKT1 tumor cells. CD532 potently inhibits Aurora A kinase activity and reduces N-Myc protein levels at sub-micromolar doses *in vitro* and substantially slows tumor growth *in vivo*. Based on these pre-clinical data, we believe that dual inhibition of N-Myc and Aurora A kinase warrants future clinical evaluation in patients with NEPC.

Lastly, the importance of N-Myc in the development of NEPC is highlighted by our prior contrasting finding that c-Myc combined with myrAKT1 in the same system generates adenosquamous carcinoma of the prostate but not NEPC (Stoyanova et al., 2013). The notion that Myc family members can drive distinct oncogenic differentiation pathways has been inferred from the amplification of specific Myc family members in several human cancers (Beltran, 2014). Compelling functional data in support of this idea has also come from a mouse model system in which the overexpression of *MYC* or *MYCN* combined with

the loss of *TP53* in mouse cerebellar neural progenitor cells produced distinct tumors akin to two different subgroups of human medulloblastoma (Kawauchi et al., 2012). The differential regulation of Myc transcriptional programs in human cancers and the mechanisms by which N-Myc initiates a neuroendocrine transformation program in prostate cancer warrant further study.

EXPERIMENTAL PROCEDURES

Human Prostate Transformation Assay

De-identified human prostate tissues were obtained from the UCLA Translation Pathology Core Laboratory and are exempt from UCLA Institutional Review Board approval. The processing of human prostate tissue, acquisition of epithelial subpopulations, lentiviral transduction, recombination with mouse UGSM, and subcutaneous grafting in NSG mice were performed as previously described (Goldstein et al., 2010). Subcutaneous implantation of transduced human prostate epithelial cell and UGSM grafts was performed in accordance with a protocol approved by the Animal Research Committee at UCLA. Mice were obtained from The Jackson Laboratory and mouse care and husbandry were performed according to the regulations of the Division of Laboratory Animal Medicine at UCLA.

Lentiviral Constructs

The cloning of lentiviral constructs is described in the Supplemental Experimental Procedures.

Cell Lines

Information on cell lines and culture conditions are provided in the Supplemental Experimental Procedures.

Histology, Immunohistochemistry, and Immunoblotting

Protocols and antibodies used for histology, immunohistochemistry, and immunoblotting of tissues and cell lines are described in the Supplemental Experimental Procedures.

Castration-Resistance and Metastasis Assays

Protocols for castration-resistance and metastasis assays are provided in the Supplemental Experimental Procedures.

Whole Transcriptome Sequencing Analysis

Details regarding laser capture microdissection, RNA isolation, library preparation, RNA sequencing analysis, and generation of the neuroendocrine prostate cancer gene signature are described in the Supplemental Experimental Procedures.

Copy Number Variation and Whole Exome Sequencing Analysis

Protocols for copy number variation and whole exome sequencing analysis are presented in the Supplemental Experimental Procedures.

Serial Dilution, Clonal Subline, and N-Myc Dependence Xenograft Studies

Protocols for serial dilution, clonal subline, and N-Myc dependence xenograft studies are described in the Supplemental Experimental Procedures.

Small Molecule Inhibitors

The sources of small molecule inhibitors and protocols for *in vitro* and *in vivo* CD532 studies are provided in the Supplemental Experimental Procedures.

Supplementary Material

Refer to Web version on PubMed Central for supplementary material.

Acknowledgments

We thank Drs. Himisha Beltran and Mark Rubin at the Weill Medical College of Cornell University for sharing primary data from their human prostate cancer RNA-Seq dataset. We thank the Translational Pathology Core Laboratory at UCLA, the California NanoSystems Institute Advanced Light Microscopy and Spectroscopy Shared Resource Facility, the UCLA Clinical Microarray Core, the High Throughput Sequencing Core at the Broad Stem Cell Research Center at UCLA, and the Clinical and Molecular Cytogenetics Laboratories at UCLA for core services. We thank the Harvard Medical School LINCS Center, which is funded by NIH grants (U54 HG006097, U54 HL127365), for use of publically available KINOME*scan* data.

This research was supported by the UCLA Hal Gaba Director's Fund for Cancer Stem Cell Research. J.K.L. is supported by the Tower Cancer Research Foundation Career Development Award, a Prostate Cancer Foundation Young Investigator Award, and the UCLA Subspecialty Training and Advanced Research Program, J.W. Phillips is supported by the UCLA Tumor Cell Biology Training Grant (T32CA09056), B.A.S. is supported by the UCLA Tumor Immunology Training Grant (T32CA009120), J.W. Park is supported by a UCLA Broad Stem Cell Research Center Training Grant, and T.S. is supported by a Prostate Cancer Foundation Young Investigator Award and a NCI/NIH K99 Award (K99CA184397). W.C.G. is supported by a NIH K08 Award (K08NS079485) and the Alex's Lemonade Stand Foundation. J.H. is supported by NIH grants (5R01CA172603-02, 2P30CA016042-39, 1R01CA181242-01A1, 1R01CA195505), the Department of Defense Prostate Cancer Research Program (W81XWH-12-1-0206), UCLA SPORE in Prostate Cancer, Prostate Cancer Foundation Honorable A. David Mazzone Special Challenge Award, and UCLA Jonsson Comprehensive Cancer Center Impact Grant. K.M.S and O.N.W. are Investigators of the Howard Hughes Medical Institute. O.N.W. is supported by a NIH grant (U01 CA164188-01A) and a Prostate Cancer Foundation Challenge Award. A.S., J.M.S., K.M.S., J.H., and O.N.W. are supported by a Stand Up To Cancer/Prostate Cancer Foundation/Prostate Dream Team Translational Cancer Research Grant (SU2C-AACR-DT0812). This research grant is made possible by the generous support of the Movember Foundation. Stand Up To Cancer is a program of the Entertainment Industry Foundation administered by the American Association for Cancer Research.

REFERENCES

Beltran H. The N-myc Oncogene: Maximizing its Targets, Regulation, and Therapeutic Potential. Molecular cancer research : MCR. 2014; 12:815–822. [PubMed: 24589438]

Beltran H, Rickman DS, Park K, Chae SS, Sboner A, MacDonald TY, Wang Y, Sheikh KL, Terry S, Tagawa ST, et al. Molecular characterization of neuroendocrine prostate cancer and identification of new drug targets. Cancer discovery. 2011; 1:487–495. [PubMed: 22389870]

Beltran H, Tomlins S, Aparicio A, Arora V, Rickman D, Ayala G, Huang J, True L, Gleave ME, Soule H, et al. Aggressive variants of castration-resistant prostate cancer. Clin Cancer Res. 2014; 20:2846–2850. [PubMed: 24727321]

Berman-Booty LD, Knudsen KE. Models of neuroendocrine prostate cancer. Endocrine-related cancer. 2015; 22:R33–R49. [PubMed: 25349195]

Boutros PC, Fraser M, Harding NJ, de Borja R, Trudel D, Lalonde E, Meng A, Hennings-Yeomans PH, McPherson A, Sabelnykova VY, et al. Spatial genomic heterogeneity within localized, multifocal prostate cancer. Nature genetics. 2015

Brockmann M, Poon E, Berry T, Carstensen A, Deubzer HE, Rycak L, Jamin Y, Thway K, Robinson SP, Roels F, et al. Small molecule inhibitors of aurora-a induce proteasomal degradation of N-myc in childhood neuroblastoma. Cancer cell. 2013; 24:75–89. [PubMed: 23792191]

Carney DN, Bunn PA Jr, Gazdar AF, Pagan JA, Minna JD. Selective growth in serum-free hormone-supplemented medium of tumor cells obtained by biopsy from patients with small cell carcinoma of the lung. Proc Natl Acad Sci U S A. 1981; 78:3185–3189. [PubMed: 6265940]

Choi N, Zhang B, Zhang L, Ittmann M, Xin L. Adult murine prostate basal and luminal cells are self-sustained lineages that can both serve as targets for prostate cancer initiation. Cancer cell. 2012; 21:253–265. [PubMed: 22340597]

Chong JA, Tapia-Ramirez J, Kim S, Toledo-Aral JJ, Zheng Y, Boutros MC, Altshuller YM, Frohman MA, Kraner SD, Mandel G. REST: a mammalian silencer protein that restricts sodium channel gene expression to neurons. Cell. 1995; 80:949–957. [PubMed: 7697725]

Clermont PL, Lin D, Crea F, Wu R, Xue H, Wang Y, Thu KL, Lam WL, Collins CC, Wang Y, et al. Polycomb-mediated silencing in neuroendocrine prostate cancer. Clin Epigenetics. 2015; 7:40. [PubMed: 25859291]

Dang CV. MYC on the path to cancer. Cell. 2012; 149:22–35. [PubMed: 22464321]

Epstein JI, Amin MB, Beltran H, Lotan TL, Mosquera J-M, Reuter VE, Robinson BD, Troncoso P, Rubin MA. Proposed Morphologic Classification of Prostate Cancer With Neuroendocrine Differentiation. The American journal of surgical pathology. 2014; 38:756–767. [PubMed: 24705311]

Fleming WH, Hamel A, MacDonald R, Ramsey E, Pettigrew NM, Johnston B, Dodd JG, Matusik RJ. Expression of the c-myc protooncogene in human prostatic carcinoma and benign prostatic hyperplasia. Cancer research. 1986; 46:1535–1538. [PubMed: 2417706]

Gao L, Schwartzman J, Gibbs A, Lisac R, Kleinschmidt R, Wilmot B, Bottomly D, Coleman I, Nelson P, McWeeney S, et al. Androgen receptor promotes ligand-independent prostate cancer progression through c-Myc upregulation. PloS one. 2013; 8:e63563. [PubMed: 23704919]

Goldstein AS, Huang J, Guo C, Garraway IP, Witte ON. Identification of a cell of origin for human prostate cancer. Science (New York, NY). 2010; 329:568–571.

Goldstein AS, Lawson DA, Cheng D, Sun W, Garraway IP, Witte ON. Trop2 identifies a subpopulation of murine and human prostate basal cells with stem cell characteristics. Proceedings of the National Academy of Sciences of the United States of America. 2008; 105:20882–20887. [PubMed: 19088204]

Grasso CS, Wu YM, Robinson DR, Cao X, Dhanasekaran SM, Khan AP, Quist MJ, Jing X, Lonigro RJ, Brenner JC, et al. The mutational landscape of lethal castration-resistant prostate cancer. Nature. 2012; 487:239–243. [PubMed: 22722839]

Gray IC, Stewart LM, Phillips SM, Hamilton JA, Gray NE, Watson GJ, Spurr NK, Snary D. Mutation and expression analysis of the putative prostate tumour-suppressor gene PTEN. British journal of cancer. 1998; 78:1296–1300. [PubMed: 9823969]

Gustafson WC, Meyerowitz JG, Nekritz EA, Chen J, Benes C, Charron E, Simonds EF, Seeger R, Matthay KK, Hertz NT, et al. Drugging MYCN through an allosteric transition in Aurora kinase A. Cancer cell. 2014; 26:414–427. [PubMed: 25175806]

Hansel DE, Nakayama M, Luo J, Abukhdeir AM, Park BH, Bieberich CJ, Hicks JL, Eisenberger M, Nelson WG, Mostwin JL, et al. Shared TP53 gene mutation in morphologically and phenotypically distinct concurrent primary small cell neuroendocrine carcinoma and adenocarcinoma of the prostate. The Prostate. 2009; 69:603–609. [PubMed: 19125417]

Helpap B, Kollermann J, Oehler U. Neuroendocrine differentiation in prostatic carcinomas: histogenesis, biology, clinical relevance, and future therapeutical perspectives. Urologia internationalis. 1999; 62:133–138. [PubMed: 10529661]

Hu Y, Smyth GK. ELDA: extreme limiting dilution analysis for comparing depleted and enriched populations in stem cell and other assays. Journal of immunological methods. 2009; 347:70–78. [PubMed: 19567251]

Huang M, Weiss WA. Neuroblastoma and MYCN. Cold Spring Harbor perspectives in medicine. 2013; 3:a014415. [PubMed: 24086065]

Jain M, Arvanitis C, Chu K, Dewey W, Leonhardt E, Trinh M, Sundberg CD, Bishop JM, Felsher DW. Sustained loss of a neoplastic phenotype by brief inactivation of MYC. Science (New York, NY). 2002; 297:102–104.

Jenkins RB, Qian J, Lieber MM, Bostwick DG. Detection of c-myc oncogene amplification and chromosomal anomalies in metastatic prostatic carcinoma by fluorescence in situ hybridization. Cancer research. 1997; 57:524–531. [PubMed: 9012485]

Karaman MW, Herrgard S, Treiber DK, Gallant P, Atteridge CE, Campbell BT, Chan KW, Ciceri P, Davis MI, Edeen PT, et al. A quantitative analysis of kinase inhibitor selectivity. Nature biotechnology. 2008; 26:127–132.

Karthaus WR, Iaquinta PJ, Drost J, Gracanin A, van Boxtel R, Wongvipat J, Dowling CM, Gao D, Begthel H, Sachs N, et al. Identification of multipotent luminal progenitor cells in human prostate organoid cultures. Cell. 2014; 159:163–175. [PubMed: 25201529]

Kawauchi D, Robinson G, Uziel T, Gibson P, Rehg J, Gao C, Finkelstein D, Qu C, Pounds S, Ellison DW, et al. A mouse model of the most aggressive subgroup of human medulloblastoma. Cancer cell. 2012; 21:168–180. [PubMed: 22340591]

Lin D, Wyatt AW, Xue H, Wang Y, Dong X, Haegert A, Wu R, Brahmbhatt S, Mo F, Jong L, et al. High fidelity patient-derived xenografts for accelerating prostate cancer discovery and drug development. Cancer Res. 2014; 74:1272–1283. [PubMed: 24356420]

Mirosevich J, Gao N, Gupta A, Shappell SB, Jove R, Matusik RJ. Expression and role of Foxa proteins in prostate cancer. The Prostate. 2006; 66:1013–1028. [PubMed: 16001449]

Mosquera JM, Beltran H, Park K, MacDonald TY, Robinson BD, Tagawa ST, Perner S, Bismar TA, Erbersdobler A, Dhir R, et al. Concurrent AURKA and MYCN gene amplifications are harbingers of lethal treatment-related neuroendocrine prostate cancer. Neoplasia. 2013; 15:1–10. [PubMed: 23358695]

Ni M, Chen Y, Fei T, Li D, Lim E, Liu XS, Brown M. Amplitude modulation of androgen signaling by c-MYC. Genes & development. 2013; 27:734–748. [PubMed: 23530127]

Otto T, Horn S, Brockmann M, Eilers U, Schuttrumpf L, Popov N, Kenney AM, Schulte JH, Beijersbergen R, Christiansen H, et al. Stabilization of N-Myc is a critical function of Aurora A in human neuroblastoma. Cancer cell. 2009; 15:67–78. [PubMed: 19111882]

Rapa I, Ceppi P, Bollito E, Rosas R, Cappia S, Bacillo E, Porpiglia F, Berruti A, Papotti M, Volante M. Human ASH1 expression in prostate cancer with neuroendocrine differentiation. Modern pathology : an official journal of the United States and Canadian Academy of Pathology, Inc. 2008; 21:700–707.

Shen H, Powers N, Saini N, Comstock CE, Sharma A, Weaver K, Revelo MP, Gerald W, Williams E, Jessen WJ, et al. The SWI/SNF ATPase Brm is a gatekeeper of proliferative control in prostate cancer. Cancer research. 2008; 68:10154–10162. [PubMed: 19074882]

Shen R, Dorai T, Szaboles M, Katz AE, Olsson CA, Buttyan R. Transdifferentiation of cultured human prostate cancer cells to a neuroendocrine cell phenotype in a hormone-depleted medium. Urol Oncol. 1997; 3:67–75. [PubMed: 21227062]

Spiess PE, Pettaway CA, Vakar-Lopez F, Kassouf W, Wang X, Busby JE, Do KA, Davuluri R, Tannir NM. Treatment outcomes of small cell carcinoma of the prostate: a single-center study. Cancer. 2007; 110:1729–1737. [PubMed: 17786954]

Stephenson RA, Dinney CP, Gohji K, Ordonez NG, Killion JJ, Fidler IJ. Metastatic model for human prostate cancer using orthotopic implantation in nude mice. Journal of the National Cancer Institute. 1992; 84:951–957. [PubMed: 1378502]

Stoyanova T, Cooper AR, Drake JM, Liu X, Armstrong AJ, Pienta KJ, Zhang H, Kohn DB, Huang J, Witte ON, et al. Prostate cancer originating in basal cells progresses to adenocarcinoma propagated by luminal-like cells. Proceedings of the National Academy of Sciences of the United States of America. 2013; 110:20111–20116. [PubMed: 24282295]

Sutherland KD, Proost N, Brouns I, Adriaensen D, Song JY, Berns A. Cell of origin of small cell lung cancer: inactivation of Trp53 and Rb1 in distinct cell types of adult mouse lung. Cancer cell. 2011; 19:754–764. [PubMed: 21665149]

Tan HL, Sood A, Rahimi HA, Wang W, Gupta N, Hicks J, Mosier S, Gocke CD, Epstein JI, Netto GJ, et al. Rb loss is characteristic of prostatic small cell neuroendocrine carcinoma. Clinical cancer

research : an official journal of the American Association for Cancer Research. 2014; 20:890–903. [PubMed: 24323898]

Valastyan S, Weinberg RA. Tumor metastasis: molecular insights and evolving paradigms. Cell. 2011; 147:275–292. [PubMed: 22000009]

Wang W, Epstein JI. Small cell carcinoma of the prostate. A morphologic and immunohistochemical study of 95 cases. The American journal of surgical pathology. 2008; 32:65–71. [PubMed: 18162772]

Wang X, Julio MK-d, Economides KD, Walker D, Yu H, Halili MV, Hu Y-P, Price SM, Abate-Shen C, Shen MM. A luminal epithelial stem cell that is a cell of origin for prostate cancer. Nature. 2009; 461:495–500. [PubMed: 19741607]

Williamson SR, Zhang S, Yao JL, Huang J, Lopez-Beltran A, Shen S, Osunkoya AO, MacLennan GT, Montironi R, Cheng L. ERG-TMPRSS2 rearrangement is shared by concurrent prostatic adenocarcinoma and prostatic small cell carcinoma and absent in small cell carcinoma of the urinary bladder: evidence supporting monoclonal origin. Modern pathology : an official journal of the United States and Canadian Academy of Pathology, Inc. 2011; 24:1120–1127.

Wu CH, van Riggelen J, Yetil A, Fan AC, Bachireddy P, Felsher DW. Cellular senescence is an important mechanism of tumor regression upon c-Myc inactivation. Proceedings of the National Academy of Sciences of the United States of America. 2007; 104:13028–13033. [PubMed: 17664422]

Wu X, Senechal K, Neshat MS, Whang YE, Sawyers CL. The PTEN/MMAC1 tumor suppressor phosphatase functions as a negative regulator of the phosphoinositide 3-kinase/Akt pathway. Proceedings of the National Academy of Sciences of the United States of America. 1998; 95:15587–15591. [PubMed: 9861013]

Yao JL, Madeb R, Bourne P, Lei J, Yang X, Tickoo S, Liu Z, Tan D, Cheng L, Hatem F, et al. Small cell carcinoma of the prostate: an immunohistochemical study. The American journal of surgical pathology. 2006; 30:705–712. [PubMed: 16723847]

SIGNIFICANCE

Our studies underscore the functional significance of the *MYCN* oncogene in NEPC. Deregulated expression of *MYCN* combined with myristoylated *AKT1* drives the development of prostate adenocarcinoma and NEPC from human prostate epithelial cells. We present direct evidence that both tumor subtypes can be derived from a common epithelial precursor. N-Myc expression is essential to maintain the tumor state, indicating that N-Myc may be a therapeutic target in *MYCN*-amplified NEPC. Pharmacologic disruption of N-Myc by the targeted inhibition of Aurora A kinase causes a marked reduction in tumor growth. In summary, we provide insight into the pathogenesis of NEPC and the rationale for a therapeutic strategy in this deadly disease.

HIGHLIGHTS

- N-Myc and AKT1 drive NEPC from human prostate epithelium
- Prostate epithelial cells can give rise to neuroendocrine and epithelial cancers
- N-Myc is essential for tumor maintenance in tumors initiated by N-Myc and AKT1
- Destabilization of N-Myc through Aurora A kinase inhibition induces tumor cell death

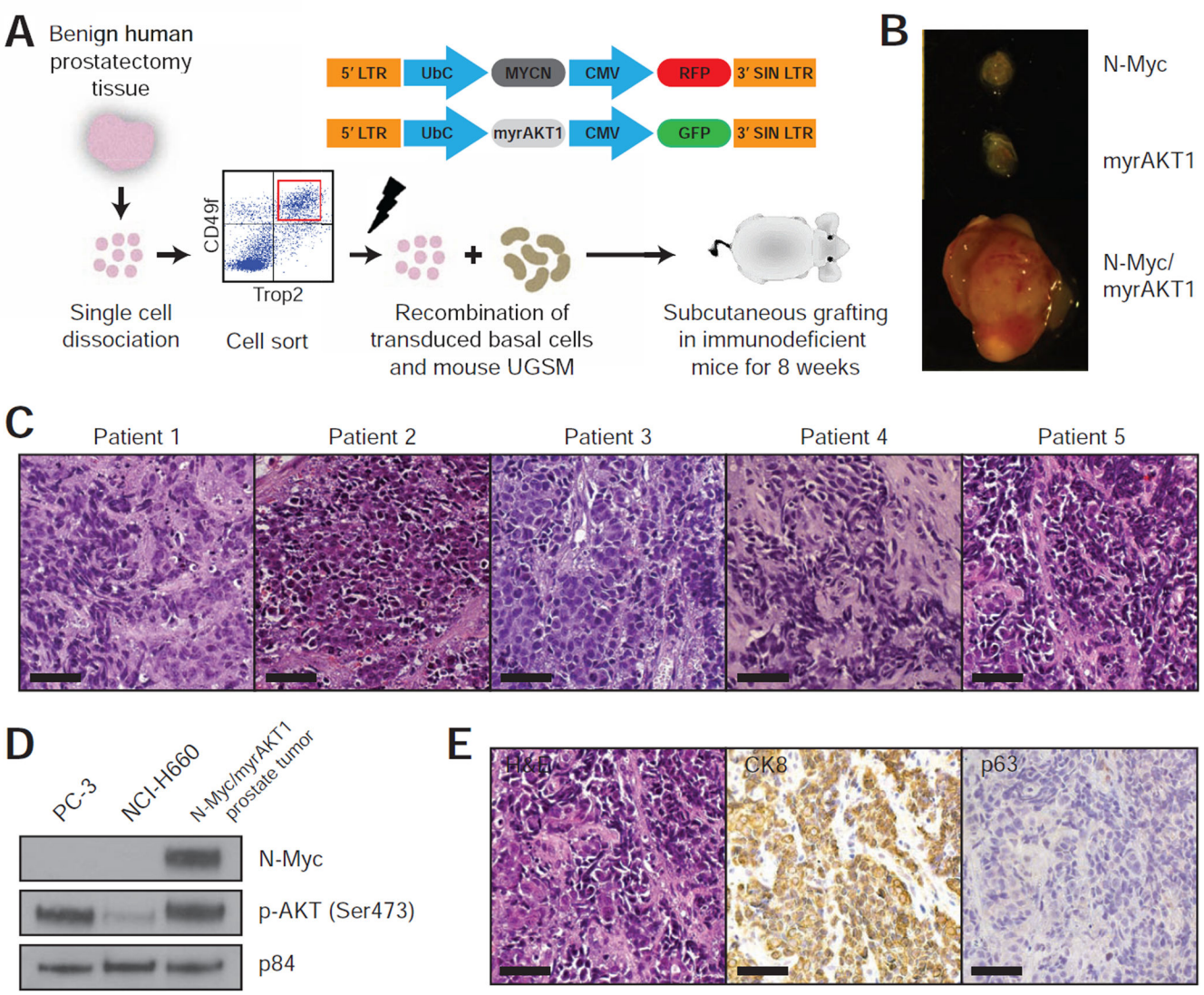

Figure 1. N-Myc and myrAKT1 initiate NEPC from human prostate basal epithelial cells

(A) Schematic of a human prostate regeneration and transformation assay (UbC=human ubiquitin C promoter, CMV=cytomegalovirus promoter, SIN=self-inactivating). The red square outlines the $Trop2^{+}CD49f^{hi}$ basal epithelial cell population. (B) Grafts transduced with N-Myc, myrAKT1, and N-Myc/myrAKT1 harvested after 8 weeks (scale bar=2 mm). (C) H&E-stained sections of N-Myc/myrAKT1 tumors derived from individual patient prostatectomy samples (scale bar=100 μm). (D) Immunoblot of the human NEPC cell lines PC-3 and NCI-H660 and an N-Myc/myrAKT1 tumor with antibodies against N-Myc, p-AKT (Ser473), and p84 as a loading control. (E) H&E and immunohistochemical stains of an N-Myc/myrAKT1 tumor for CK8 and p63 (scale bar=100 μm). See also Figure S1 and Table S1.

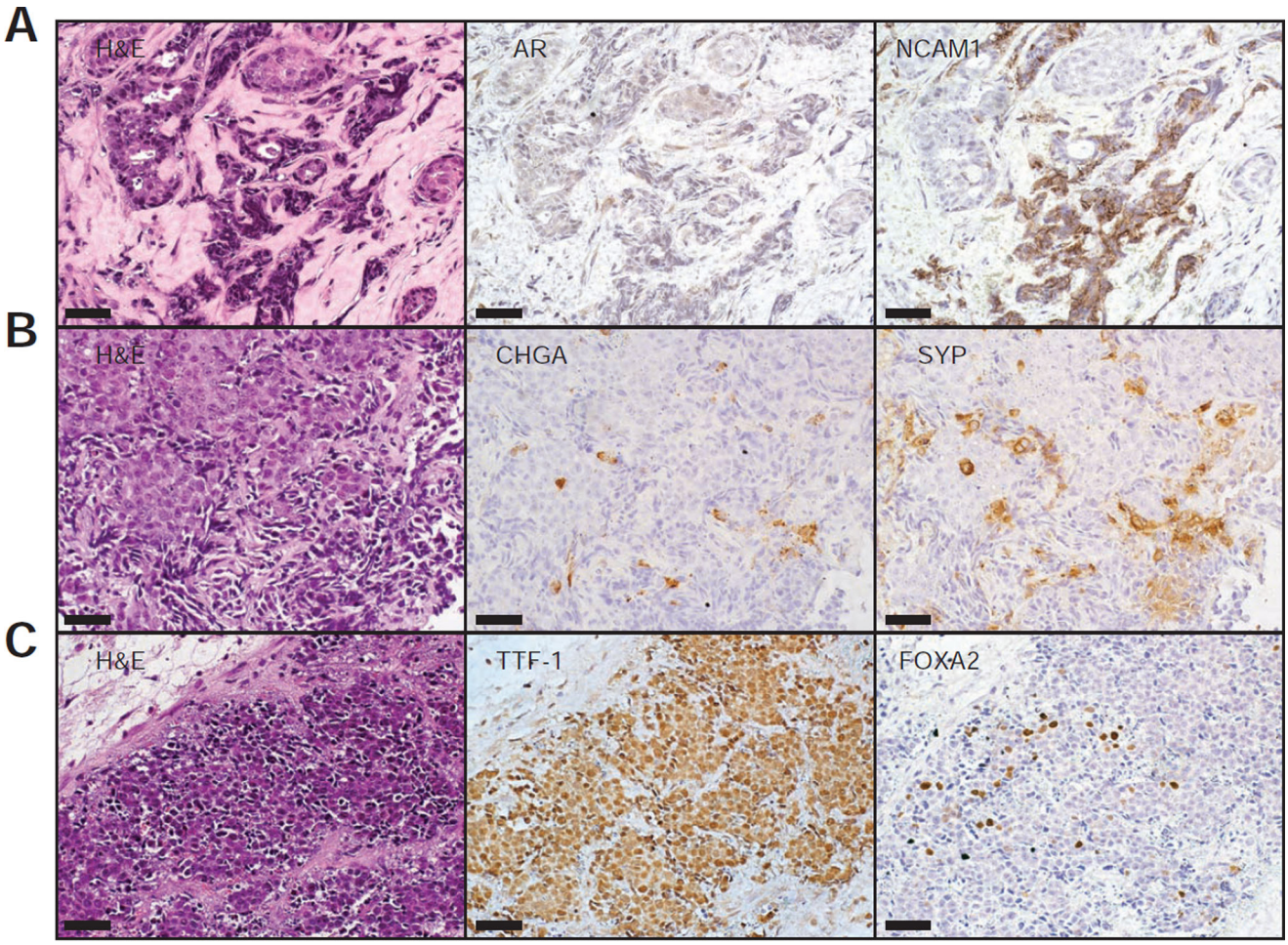

D

	AR	NCAM1	CHGA	SYP	TTF1	FOXA2
NA 1	-	+	+	+	+	+
NA 2	-	-	-	-	+	+
NA 3	-	+	-	+	-	+
NA 4	-	-	-	-	+	+
NA 5	-	+	-	-	-	+

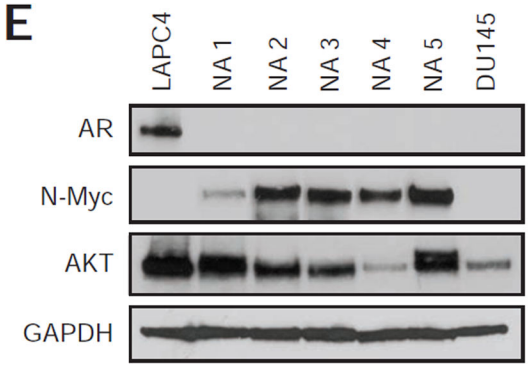

Figure 2. Prostate tumors initiated by N-Myc and myrAKT1 lack AR expression and exhibit neuroendocrine markers

(A–C) Photomicrographs of N-Myc/myrAKT1 tumor sections containing regions of neuroendocrine carcinoma with H&E stains and immunohistochemical staining for AR and NCAM1, CHGA and SYP, and TTF-1 and FOXA2 (scale bar=100 μm). (D) Summary of the immunohistochemical staining for neuroendocrine markers in the regenerated tumors derived from five independent patient prostate samples. Positive staining represents visible staining in at least 5% of the tumor cells. (E) Immunoblot of the AR-positive human prostate cancer cell line LNCaP, five different N-Myc/myrAKT1 (NA) tumors, and the AR-null

human prostate cancer cell line DU145 with antibodies against AR, N-Myc, AKT, and GAPDH as a loading control.

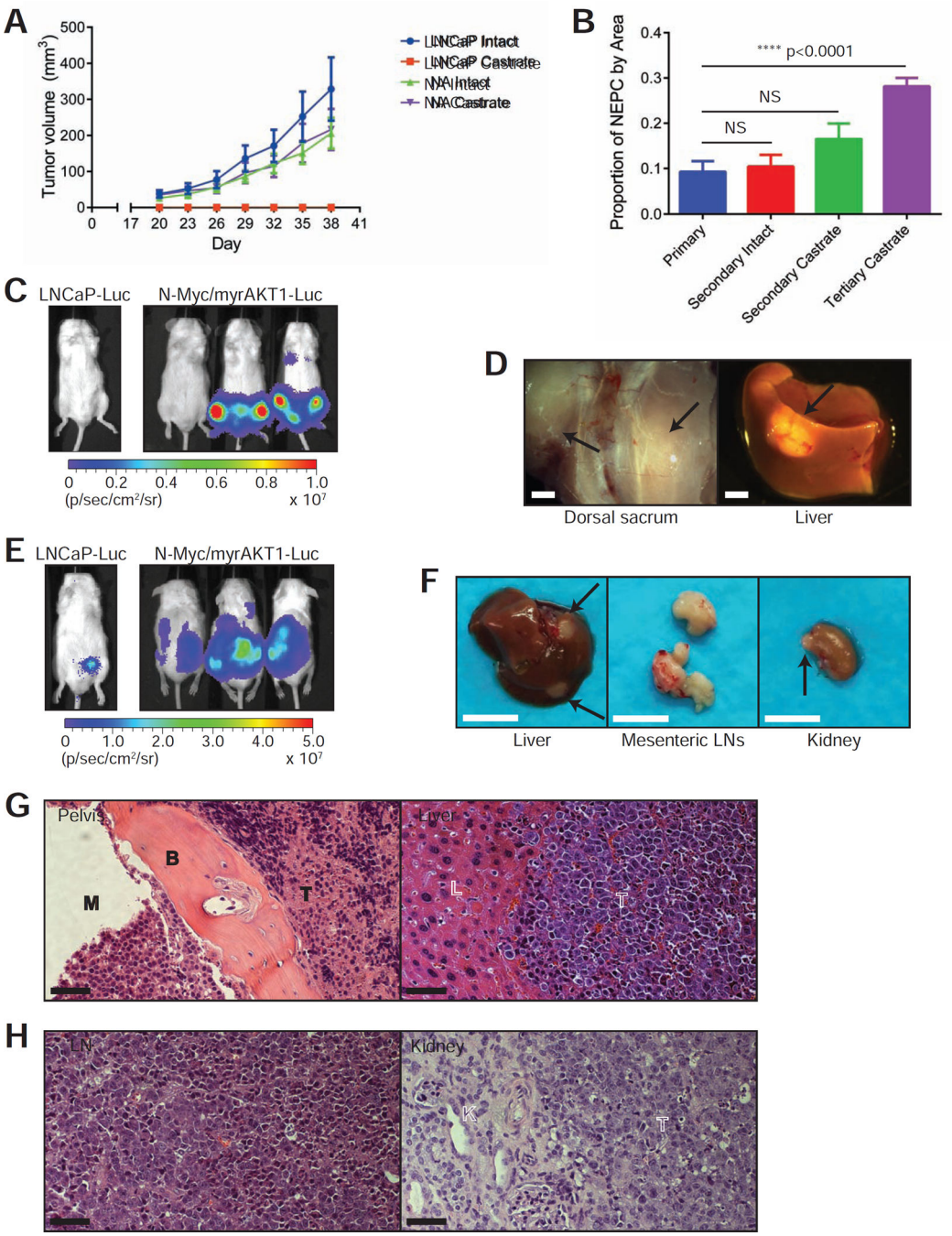

Figure 3. N-Myc/myrAKT1 prostate tumors are castration-resistant and metastasize widely

(A) LNCaP and transplanted N-Myc/myrAKT1 (NA) tumor volumes +/− SD (n=4 for each condition) in intact and surgically castrate mice over time. (B) Average percentage of neuroendocrine carcinoma identified by smart image segmentation +/− SEM in sections of primary, secondary, and tertiary N-Myc/myrAKT1 prostate tumors. p-values were calculated from an one-way analysis of variance. (C) Bioluminescent imaging of mice 21 days after tail vein injection with the LNCaP-Luc or N-Myc/myrAKT1-Luc cell lines (signal intensity is represented by radiance, p/sec/cm^2/sr). (D) Gross tumor deposits marked by closed arrows

localized to the sacrum and liver in N-Myc/myrAKT1-Luc injected mice (scale bar=2 mm). (E) Bioluminescent imaging of mice 74 days after orthotopic injection with the LNCaP-Luc or N-Myc/myrAKT1-Luc cell lines. (F) Gross metastatic tumors marked by closed arrows involving the liver, mesenteric lymph nodes (LNs), and kidney of N-Myc/myrAKT1-Luc mice (scale bar=1 cm). (G) H&E-stained sections of metastatic N-Myc/myrAKT1-Luc tumors in the pelvis and liver with M=marrow space, B=bone, L=liver, and T=tumor (scale bar=100 μm). (H) H&E-stained sections of metastatic N-Myc/myrAKT1-Luc tumors in a mesenteric LN and kidney with K=kidney and T=tumor (scale bar=100 μm). See also Figure S2.

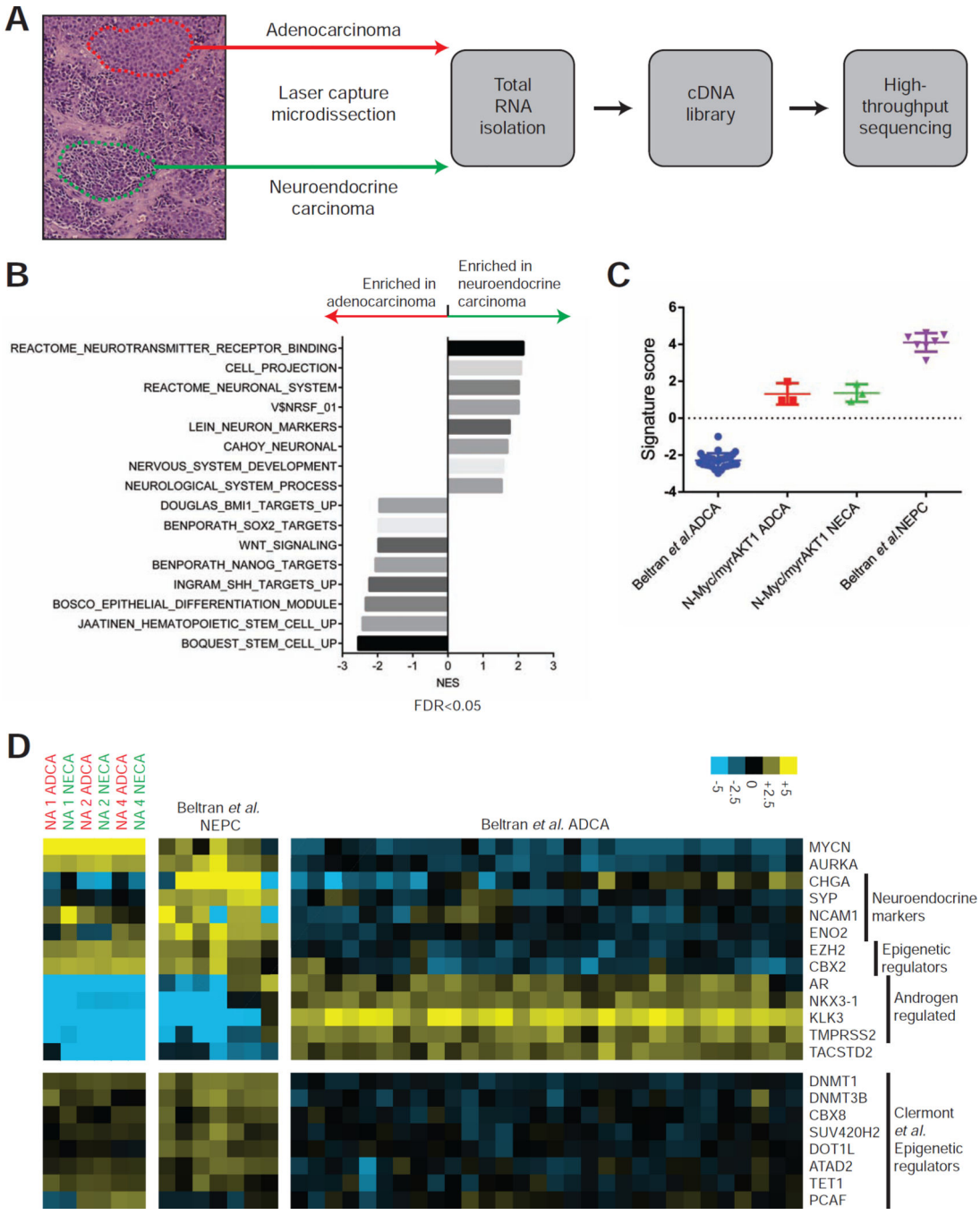

Figure 4. Transcriptome profiling of the N-Myc/myrAKT1 tumors demonstrates similarity to human NEPC

(A) Schematic of the laser capture microdissection of matched regions of adenocarcinoma and neuroendocrine carcinoma in an N-Myc/myrAKT1 tumor and the workflow for whole transcriptome shotgun sequencing. (B) Gene set enrichment analysis for genes differentially expressed (>4-fold) in the adenocarcinoma or neuroendocrine carcinoma from the N-Myc/myrAKT1 tumor derived from Patient 1. (C) Neuroendocrine prostate cancer signature scores +/− SD for Beltran *et al.* neuroendocrine prostate cancer (NEPC, n=7), N-Myc/myrAKT1 adenocarcinoma (NA ADCA, n=3), N-Myc/myrAKT1 neuroendocrine carcinoma

(NA NECA, n=3), and Beltran *et al.* adenocarcinoma (ADCA, n=30). (D) Heatmap of a selection of genes in NA ADCA, NA NECA, Beltran *et al.* NEPC, and Beltran *et al.* ADCA samples (contrast=+/−2^5). See also Figure S3 and Tables S2–S4.

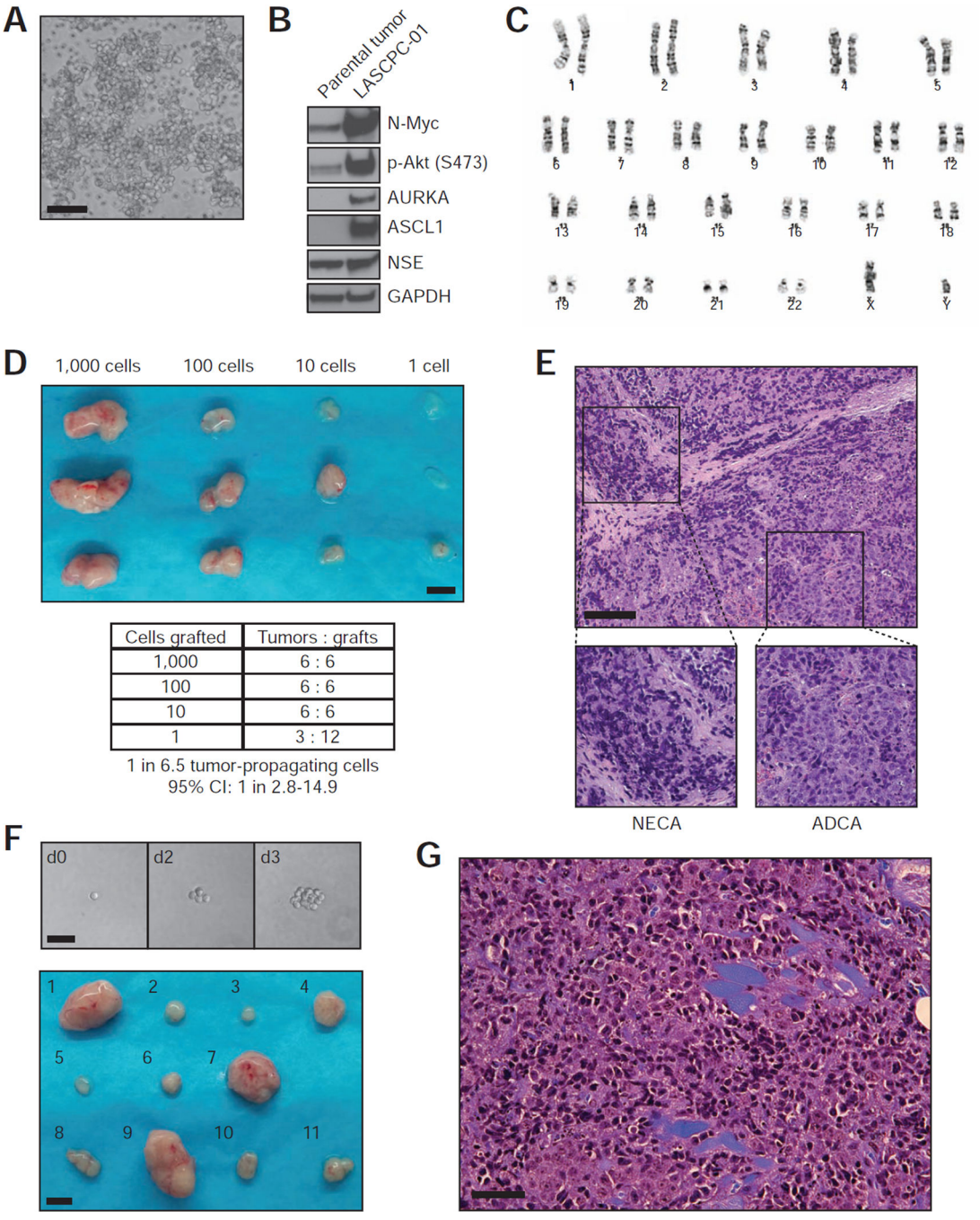

Figure 5. Establishment of a human NEPC cell line LASCPC-01 with cancer stem cell-like features

(A) Photomicrograph of the LASCPC-01 cell line growing in suspension (scale bar=100 μm). (B) Immunoblot analysis of the parental N-Myc/myrAKT1 tumor from which LASCPC-01 was derived and the LASCPC-01 cell line with antibodies against N-Myc, p-AKT (Ser473), AURKA, ASCL1, NSE, and GAPDH as a loading control. (C) Conventional karyotyping of the LASCPC-01 cell. (D) Gross tumors generated from the subcutaneous xenotransplantation of serially diluted LASCPC-01 cells after five weeks (scale bar=5 mm). (E) Representative H&E-stained section of LASCPC-01 xenograft tumors with regions of

neuroendocrine carcinoma (NECA) and adenocarcinoma (ADCA) (black scale bar=200 μm, white scale bar=100 μm). (F) Top panel, photomicrographs of LASCPC-1 cells in culture after single cell sorting, deposition, and culture (scale bar=50 μm). Bottom panel, gross tumors from the subcutaneous xenotransplantation of eleven clonal LASCPC-01 sublines after 4 weeks (scale bar=5 mm). (G) Representative H&E-stained section of a xenograft tumor derived from a clonal LASCPC-01 subline (scale bar=100 μm). See also Figure S4.

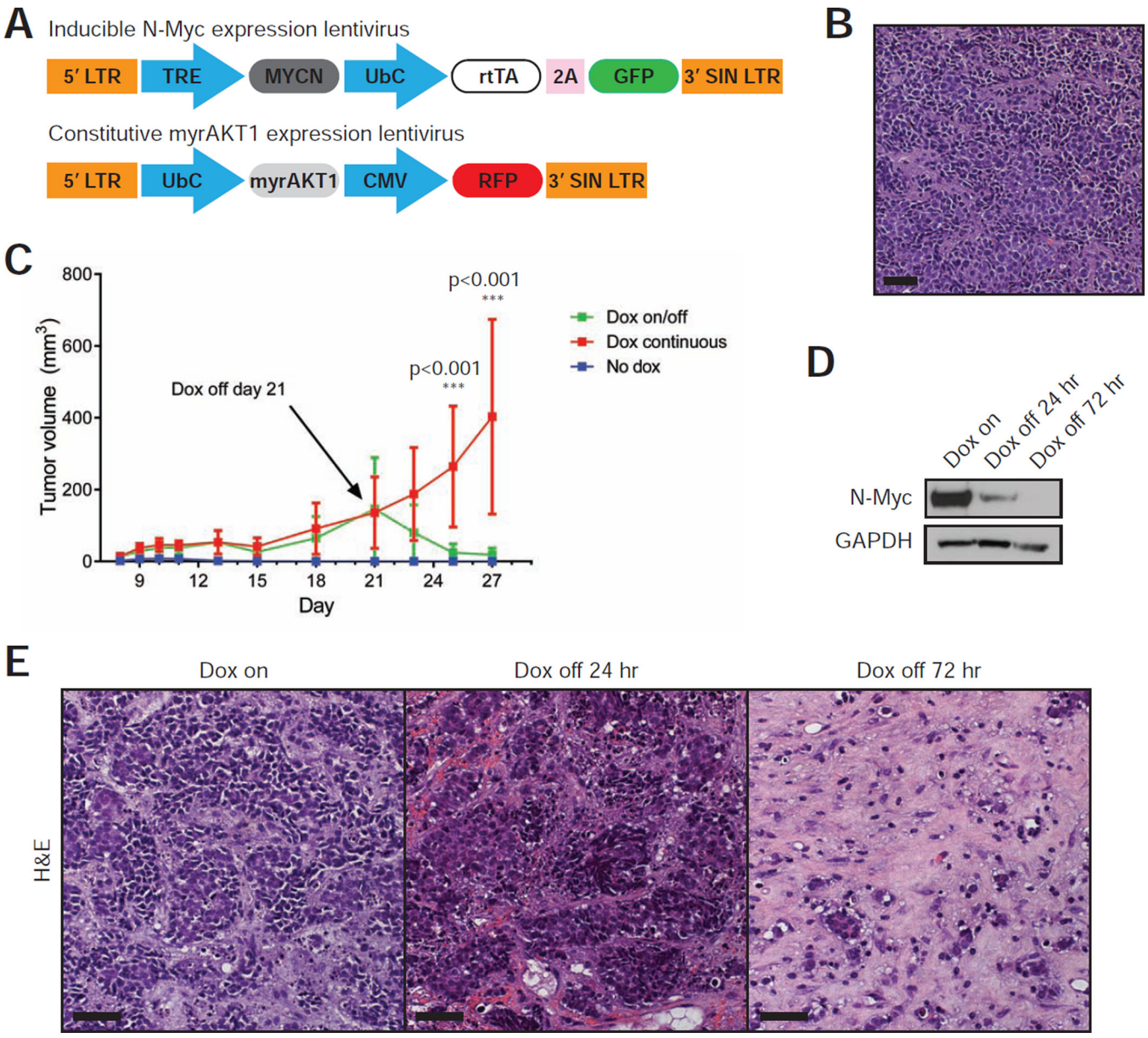

Figure 6. N-Myc expression is required for tumor maintenance in the N-Myc/myrAKTl tumors

(A) Lentiviral constructs used for doxycycline-inducible expression of N-Myc and constitutive expression of myrAKT1 (TRE=tetracycline response element, rtTA=reverse tetracycline-controlled transactivator). (B) H&E-stained section of an inducible N-Myc/myrAKT1 tumor (scale bar=100 μm). (C) Average tumor volume of passaged inducible N-Myc/myrAKT1 tumors +/− SD over time under conditions of no doxycycline (No dox, n=13), continuous doxycycline (Dox continuous, n=11), and doxycycline withdrawal on day 21 after initial doxycycline (Dox on/off, n=11). p-values were calculated from a paired t-test. (D) Immunoblot analysis of inducible N-Myc/myrAKT1 tumors after continuous doxycycline or initial doxycycline followed by withdrawal using antibodies against N-Myc and GAPDH as a loading control. (E) Representative H&E-stained sections of inducible N-

Myc/myrAKT1 tumors after continuous doxycycline and after doxycycline withdrawal (scale bar=100 μm).

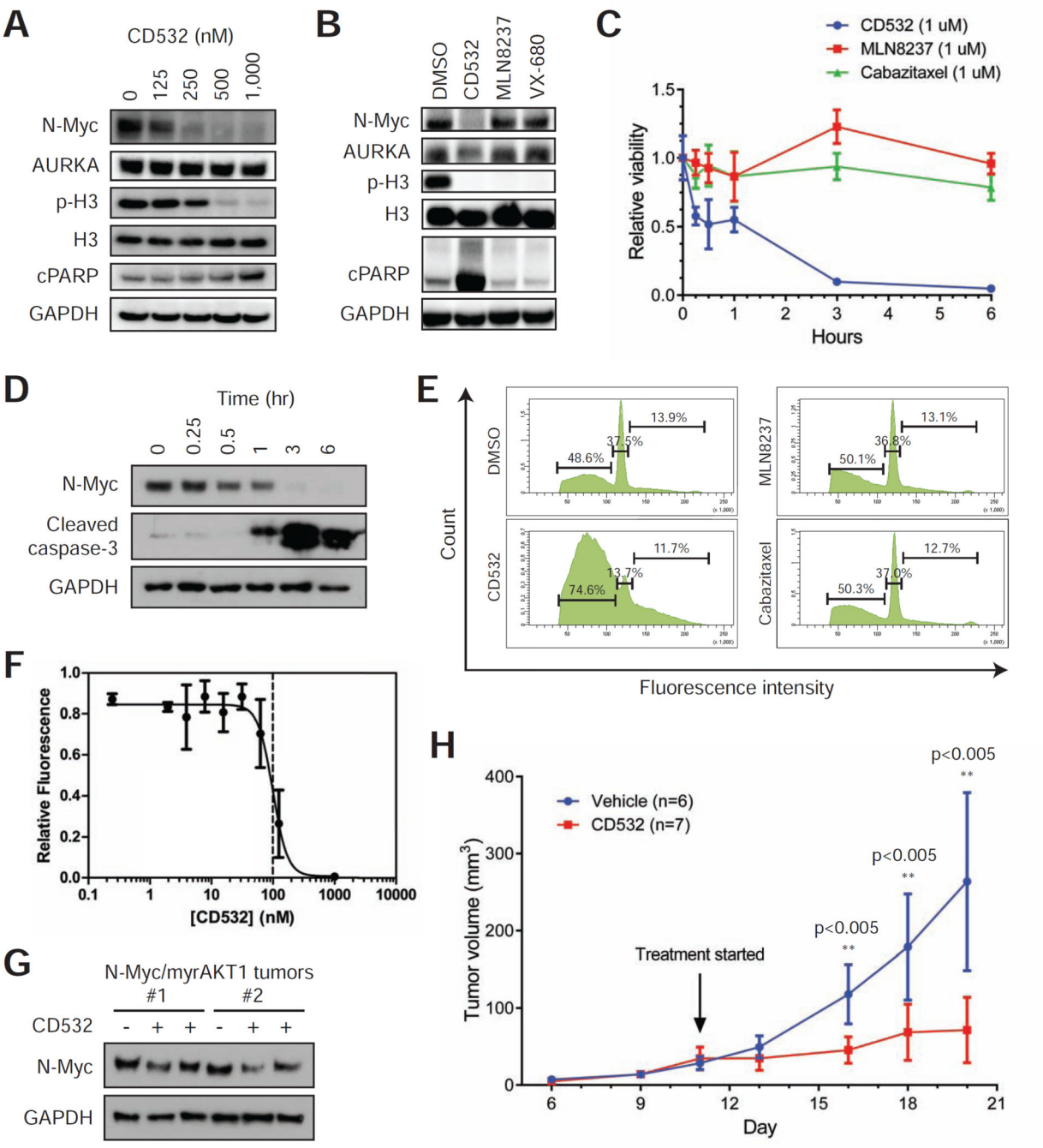

Figure 7. Therapeutic targeting of N-Myc dependence in the N-Myc/myrAKT1 model of NEPC

(A) Immunoblot analysis of LASCPC-01 cells treated with a dose range of CD532 with antibodies against N-Myc, AURKA, phosphorylated histone H3 (p-H3), histone H3, cleaved PARP (cPARP), and GAPDH as a loading control. (B) Immunoblot of LASCPC-01 treated with DMSO or 500 nM of CD532, MLN8237, or VX-680 for 3 hours with antibodies against, N-Myc, AURKA, p-H3, H3, cPARP, and GAPDH as a loading control. (C) LASCPC-01 cell viability +/− SD after 3 hours of treatment with 1 μM of CD532, MLN8237, or cabazitaxel relative to treatment with DMSO (n=6 for each condition). (D)

Immunoblot of LASCPC-01 cells treated with 1 μM of CD532 over a time course with antibodies against N-Myc, cleaved caspase-3, and GAPDH as a loading control. (E) Cell cycle analysis of LASCPC-01 cells after 3 hours of treatment with DMSO or 1 μM of CD532, MLN8237, or cabazitaxel. Quantification of the sub-G1, G1, and S/G2/M fractions is shown. (F) Dose response of CD532 +/− SD (normalized to DMSO treatment only) at 48 hours using the CellTiter-Glo cell viability assay in LASCPC-01 cells. (G) Immunoblot analysis of N-Myc/myrAKT1 tumors after treatment with vehicle or CD532 for 24 hours with antibodies against N-Myc and GAPDH as a loading control. (H) Average tumor volume of LASCPC-01 subcutaneous xenografts +/− SD with vehicle (n=6) or CD532 (n=7) treatment initiated on day 11. p-values were calculated from a paired t-test. See also Figure S5 and Table S5.